Original Article

Institution of MECHANICAL ENGINEERS
Journal of AUTOMOBILE ENGINEERING

Proc IMechE Part D:
J Automobile Engineering
2015, Vol. 229(8) 1070–1082

DOI: 10.1177/0954407014555150
pid.sagepub.com
SAGE

Experimental identification of the torque losses in V-ribbed belt drives using the response surface method

Berna Balta[1,2], Fazil O Sonmez[3] and Abdulkadir Cengiz[4]

Abstract

A drop in the transmitted torque is one of the concerns regarding the performance of belt drives, which affects the efficiency of the power transmission. In this study, the torque loss behaviour of a V-ribbed belt drive with two equal-sized pulleys is investigated using several experimental methodologies. The individual effects of belt-drive parameters are determined with the one-factor-at-a-time test method. The relation between the parameters and the torque loss is found via response surface methodology. Afterwards, the operating conditions are optimized for the minimum torque loss. A test is conducted using the optimum parameter values. The difference between the percentage torque loss predicted by the response surface curve and the experimental result is found to be 8.5%. Furthermore, the predicted model looks reasonably accurate on the basis of the analysis of variance and the residual analysis. Using the response curve, the torque loss may be estimated for similar belt drives.

Keywords

Power transmission, V-ribbed belt drives, torque loss, one-factor-at-a-time test method, response surface methodology, design optimization, analysis of variance

Date received: 8 April 2014; accepted: 17 September 2014

Introduction

About one third of electric motor transmission systems used in the industry utilize belt transmissions.[1] Different types of belt are used in the industry, e.g. flat belts, V-belts and V-ribbed belts; the V-ribbed belt can be considered to be a hybrid of the V-belt and the flat belt, thereby offering the flexibility of a flat belt combined with the power transmission capacity of a V-belt. It consists of a layer of reinforcing cords as the tension-carrying members, a protective cushion rubber that envelopes the cords, a rubber backing and ribs made of short-fibre-reinforced rubber (Figure 1).

In belt drives, power losses occur owing to a combination of speed losses and torque losses. The speed loss is due to sliding of the belt relative to the pulley, which occurs because of a number of factors such as creep along the belt, radial compliance, shear deflection and seating or unseating because of flexural stiffness.[3] The difference between the driver torque and the driven torque in a belt drive is defined as the torque loss. Torque losses include hysteresis losses, friction losses and idling losses. Hysteresis losses arise because of the bending and unbending of the belt as it enters and leaves the pulley and because of the tension differences between the slack side and the tight side. Frictional losses occur owing to sliding between the belt and the pulley. Idling losses are mainly associated with the loss of kinetic energy due to the resistance of the surrounding air to the motion of the belt.[1] With a proper design, power losses can be reduced and thus the efficiency of a belt drive can be increased, but this requires fundamental understanding of the effects of the dominant factors on the power loss.

Experimental investigations on the power losses of belt drives have mainly focused on V-belts and continuously variable transmission (CVT) belt drives. Studies

[1]Department of Mechanical Engineering, Kocaeli University, Kocaeli, Turkey
[2]Product Development Department, Ford Otosan, Gölcük, Turkey
[3]Department of Mechanical Engineering, Bogazici University, Istanbul, Turkey
[4]Mechanical Education Department, Kocaeli University, Kocaeli, Turkey

Corresponding author:
Fazil O Sonmez, Department of Mechanical Engineering, Bogazici University, Bebek 34342, Istanbul,Turkey.
Email: sonmezfa@boun.edu.tr

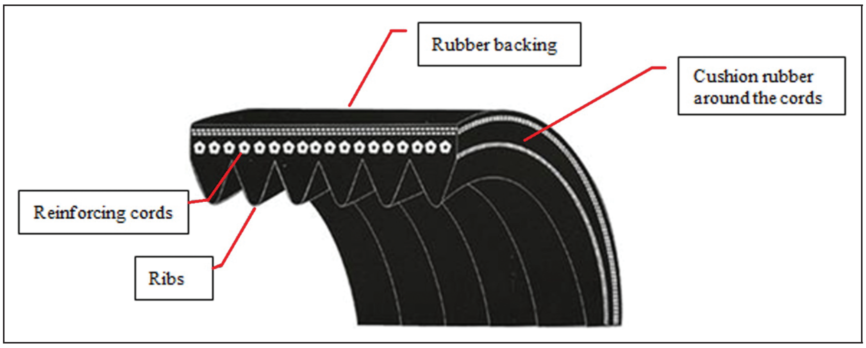

Figure 1. A typical V-ribbed belt.[2]

on the power loss behaviour of V-ribbed belt drives are fairly new. Furthermore, these studies considered mostly belt slip losses, rather than torque losses. Belt-drive test rigs with two equal-sized pulleys were the basic set-up used in those studies. Peek and Fischer[4] developed a V-belt-drive test set-up to determine the V-belt-drive efficiency for a torque of up to 200 N m and a speed of 6000 r/min with a fixed shaft distance. The belt pre-tension was provided by a pivoted rocking arm. They obtained the relationship of the braking torque versus the slip and power loss for narrow V-belt drives for a single combination of the belt tension, the belt length and the pulley diameter.

Childs and Cowburn[5] investigated the effects of the mismatch between the wedge angles of the pulley grooves and the belt ribs on the power loss behaviour of V-belt drives using a two-equal-sized-pulley test bench. During the tests, they kept the other parameters constant. They also analysed both theoretically and experimentally the effects of small pulleys on the power loss.[6] Using pulleys with diameters ranging from 42 mm to 102 mm, they examined the effect of the braking torque on the power loss. However, different belt lengths and belt materials were not considered in their study.

Several studies were conducted to investigate the CVT-type belt drives used in motorcycles with the help of belt-drive test rigs with two pulleys. Ferrando et al.[7] developed a test set-up in which an electric motor was used to run the driver pulley, and a velocity controller was used to maintain its speed. Another motor was used to apply the braking torque to the driven pulley. The belt tension, the input torque and the axial force on the moveable plate of the pulley were measured. Amijma et al.[8] investigated the effects of acceleration and deceleration on the power transmission in a CVT belt drive by measuring the axial forces at a constant speed (2430 r/min) and a constant braking torque via a load cell. Chen et al.[9] focused on the efficiency of a rubber V-belt CVT drive. In the test set-up, the input and output torques were measured with torque transducers, and the speed was measured with optical encoders. Additionally, laser displacement sensors were installed in order to detect the changes in the pitch radii of CVT pulleys and to determine the speed and torque losses under different operating conditions. Akehurst et al.[10–12] investigated the power transmission efficiency of a metal V-belt CVT drive. The belt was constructed from several hundred segments held together by steel band sets. They formulated the torque loss and belt-slip losses and correlated them with the experimental results. They concluded that the primary torque loss mechanism in the belt was due to the sliding motion which occurred between the band and the segment. They also proposed another torque loss model by considering the effects of pulley bending and deformation (i.e. pulley wedging and penetration loses) and validated the model with experimental results.

Analytical models for torque losses were previously developed for V-belt drives. Gerbert[3] analytically formulated the torque loss in V-belt drives by considering the radial compliance, the flexural rigidity and the bending stiffness of the belt. Childs and Cowburn[6] proposed a model for the torque loss behaviour in V-belt drives by taking into account the belt bending stiffness, the pulley diameter and the belt pre-tension for friction coefficients less than 0.4. The studies on the torque loss behaviour of flat and V-belt belt drives are limited and, in those studies, only a small number of belt-drive parameters were considered; the effects of the belt length and the motor speed were not determined.

Previous studies have focused on V-belt drives and V-belt CVT drives until V-ribbed belt drives were introduced in the last decade or so. For this reason, there have been relatively few published papers on V-ribbed belt drives, and those that have appeared have dealt with only belt slip losses.[13–18] The torque loss behaviour of V-ribbed belts has not been studied.

The main objective of the present study is to investigate experimentally the effects of the belt-drive parameters on the torque loss behaviour of V-ribbed belt drives. For this purpose, a test bench was built to measure the torque losses in a V-ribbed belt-drive system with two equal-sized pulleys. In comparison with the previous studies on the power loss behaviour of belt drives, a much larger number of parameters and their interactions are considered, which include the belt tension, the driver pulley speed, the braking torque, the belt length, the pulley diameter and the belt material.

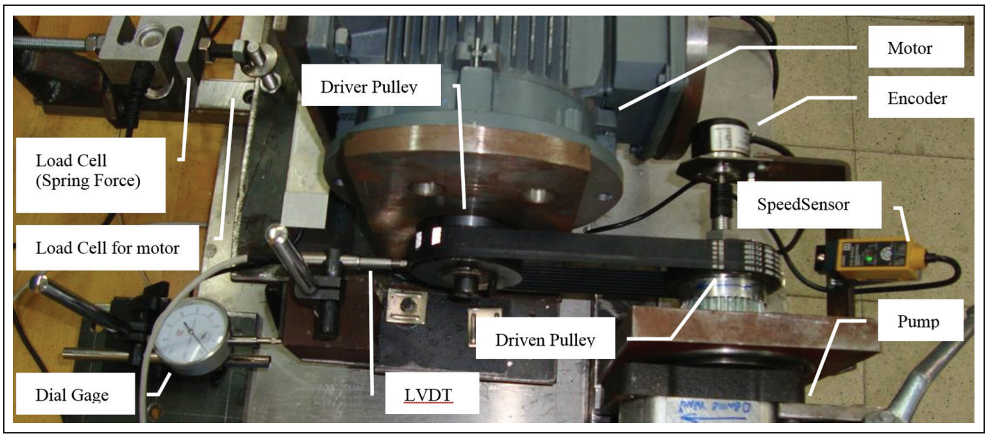

Figure 2. The experimental set-up.
LVDT: linear variable differential transformer.

The effects of the belt length and the pulley diameter on the transmission losses of V-ribbed belt drives are investigated for the first time. The effects of the individual parameters are determined using one-factor-at-a-time (OFAT) testing methodology. Furthermore, the relation between the input parameters and the torque loss is obtained using response surface methodology (RSM). Then, the optimum operating conditions are determined for the minimum torque loss via an optimization procedure.

Experimental study

Experimental set-up and instrumentation

The set-up shown in Figure 2 and schematically illustrated in Figure 3 is constructed to investigate the effects of various parameters on the torque loss behaviour of V-ribbed belt drives. J-type V-ribbed belts with four ribs are used for transmitting power between the pulleys. The belt drive is actuated by an asynchronous electric motor with a maximum power output of 3 kW, which is driven via a frequency inverter used to adjust the angular velocity of the driver pulley. The braking torque applied to the driven pulley is provided by a hydraulic pump, which serves as a dynamometer. It can be run in different steady-state operating conditions by means of a valve, and thus different magnitudes of braking torque can be applied to the belt drive. The maximum braking torque capacity is 10 N m, beyond which localized slip behaviour turns into gross slip. The controllable input parameters and the measured parameters are summarized in Table 1.

In order to be able to modify the belt tension and to accommodate different pulley diameters and belt lengths, the motor is located on a sliding base. Pre-tension is induced by means of a spring mechanism, which applies a spring force to the sliding base. The sum of the tension in the tight side of the belt and the tension in the slack side of the belt is measured with a load cell. The motor and dynamometer are mounted on two different sets of ball-bearing housings. The magnitudes of the reaction forces causing the driving torque and the driven torque are measured using two other load cells, which are mounted on the motor housing and the dynamometer housing respectively. The angular speed of the driver pulley is measured with an optical encoder. Additionally, a photoelectric switch is installed to count the belt rotation in order to check the accuracy of the measurements of the encoder. The measurements obtained with the encoder and the photoelectric switch turned out to be in good agreement. The differences can be attributed to slip between the belt and the pulley. In order to measure the centre distance between the pulleys, a dial gauge is placed on the sliding base on which the motor is mounted.

The data measured with the encoders, photoelectric switch and load cells are processed in the microprocessors to be converted to digital data; then they are transferred to the computer using the data acquisition software LabVIEW™.

Measuring torque losses

After the V-ribbed belt is installed on the pulleys, they are pulled apart until a specific belt tension is induced. The driver pulley, rotated by the motor, actuates the belt, which in turn rotates the driven pulley, while the dynamometer applies the braking load to the belt-drive system. The torques acting on the housings of the motor and the dynamometer are measured using load cells. M_1^* and M_2^* denote the measured torque on the motor housing and the measured torque on the dynamometer housings respectively. In order to determine the net torques directly acting on the driver pulley and the driven pulley accurately, the idling torque losses M_i occurring at the motor and the dynamometer should be subtracted from the measured torque values M_i^*. In order to obtain the idling torque losses, the belt is disassembled, the motor is run and the torque generated at the motor housing is

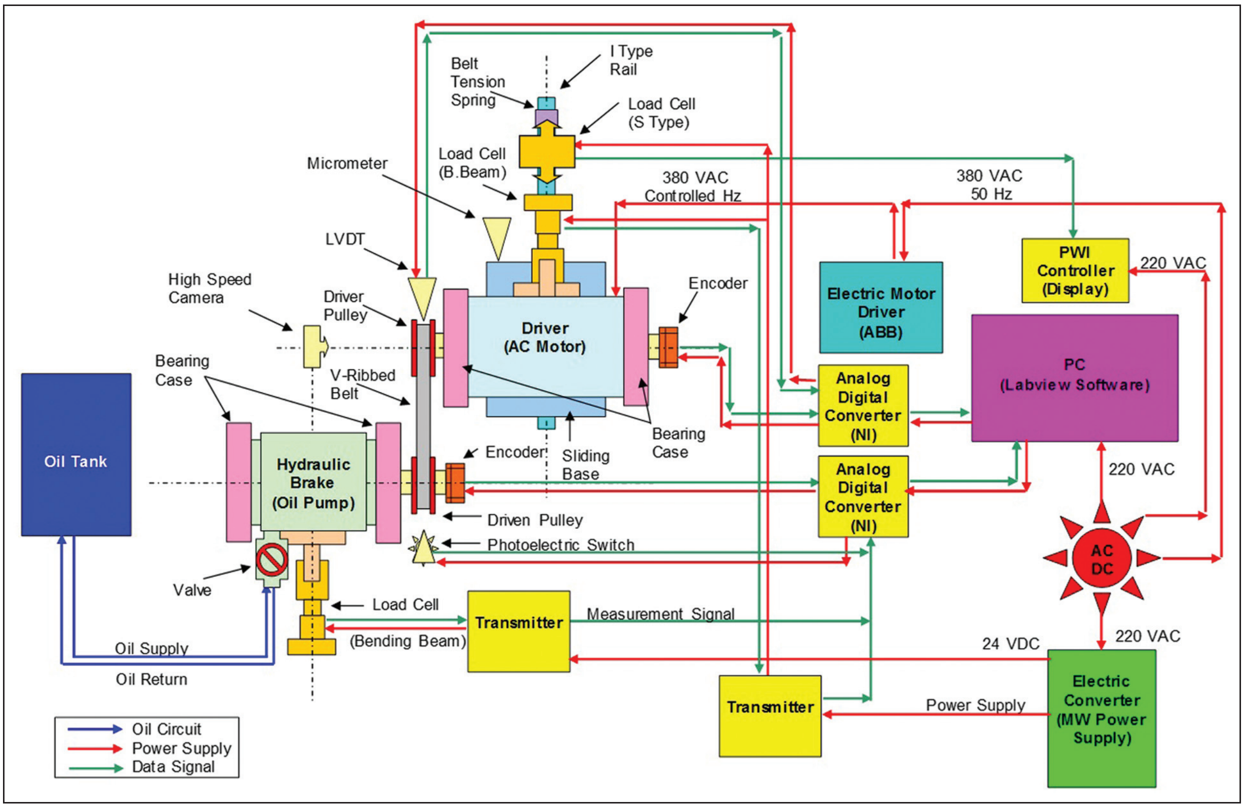

Figure 3. Schematic diagram of the experimental set-up and the instruments.
AC: a.c.; LVDT: linear variable differential transformer; PWI: PowerWise Interface™; NI: National Instruments; PC: personal computer; DC: d.c.

Table 1. The test parameters.

Input parameters of the system	Measured parameters of the system
Motor speed	Angular speeds of the pulleys
Braking torque	Driver torque
Belt pre-tension	Braking torque
Belt length	Belt pre-tension
Pulley diameter	Belt length
Belt material	Belt specific speed
	Centre distance

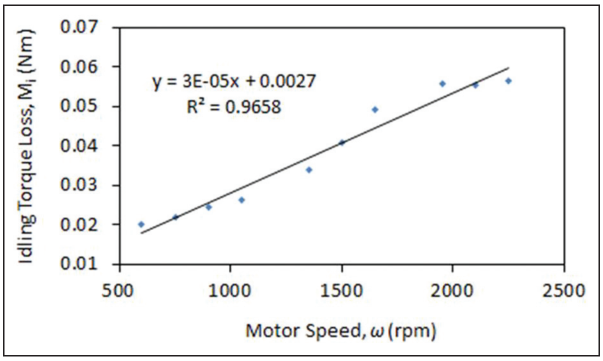

Figure 4. Idling torque losses at the motor.

measured. Figure 4 shows the idling torque losses as a function of the motor speed.[19]

The best-fitting equation for the idling losses is found to be

$$M_i = 3\times10^{-5}\omega + 0.0027 \tag{1}$$

where the idling torque M_i is in newton metres and ω is in revolutions per minute. The net torque M_1 on the driver pulley and the net torque M_2 on the driven pulley are defined as

$$M_1 = M_1^* - M_i \tag{2}$$

and

$$M_2 = M_2^* - M_i \tag{3}$$

respectively. Here, considering that the driver pulley and the driven pulley are rotated at about the same speed, the torque losses due to air resistance are assumed to be the same. Also, the torque losses due to friction at the bearings of the motor housing and the dynamometer housing are neglected. Hence, the percentage torque loss is evaluated as

$$\Delta M(\%) = \frac{M_1 - M_2}{M_1}\times100 \tag{4}$$

One-factor-at-a-time test results

In order to identify the parameters affecting the percentage torque loss and to demonstrate their individual

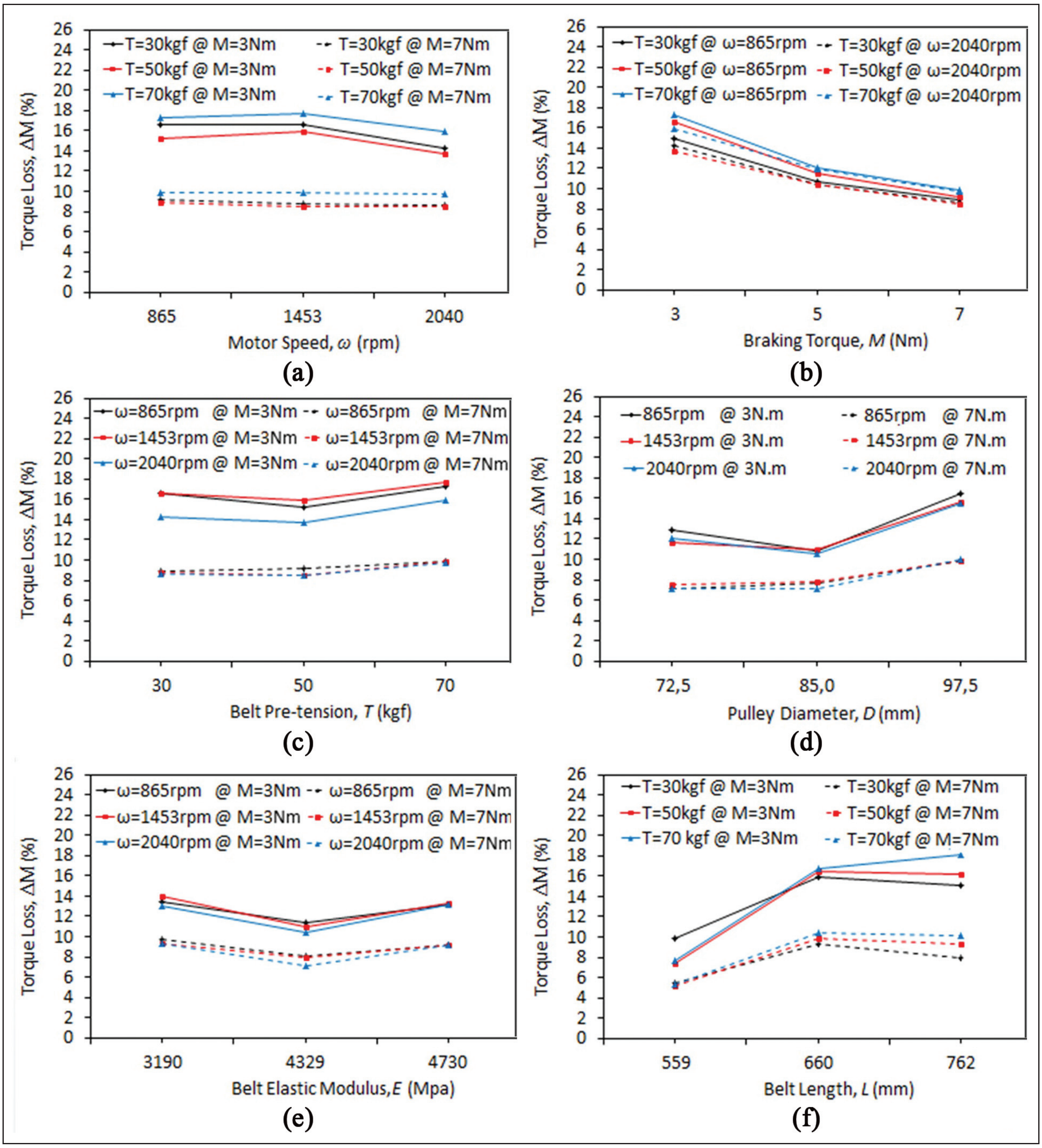

Figure 5. The relation between the percentage torque loss ΔM (%) and the input parameters: (a) the braking torque M ($E = 3190$ MPa; $L = 559$ mm; $D = 72.5$ mm); (b) the driver pulley speed ω ($E = 3190$ MPa; $L = 559$ mm; $D = 72.5$ mm); (c) the belt tension T ($E = 3190$ MPa; $L = 559$ mm: $D = 72.5$ mm); (d) pulley diameter D ($E = 4730$ MPa; $L = 660$ mm; $T = 50$ kgf); (e) the elastic modulus E of the belt ($L = 559$ mm; $T = 50$ kgf; $D = 85$ mm); (f) the belt length L ($E = 4730$ MPa; $\omega = 865$ r/min; $D = 97.5$ mm).

effects, OFAT tests are conducted, in which one parameter is changed at a time. The elastic modulus is assumed to be the only property of the belt material that affects the torque loss behaviour. Accordingly, the elastic modulus is directly taken as a belt-drive parameter. The results are shown in Figure 5.

In Figure 5(a), the percentage torque loss $\Delta M(\%)$ is given as a function of the driver pulley speed ω. At high braking torques, $\Delta M(\%)$ remains nearly constant for various pulley speeds. At low braking torques, $\Delta M(\%)$ first slightly increases and then drops with increasing speed.

As indicated in Figure 5(b), $\Delta M(\%)$ decreases when the braking torque is increased regardless of the belt tension and the speed. In fact, the absolute torque loss slightly increases with increasing braking torque. This is because the difference between the tension in the slack side and the tension in the tight side increases with increased braking torque; this, in turn, exacerbates the hysteresis effect associated with longitudinal stretching and contraction of the belt. This effect, nevertheless, does not increase as much as the braking torque. As a result, $\Delta M(\%)$ shows a decreasing trend with increasing braking torque.

$\Delta M(\%)$ shows a little increase with increasing belt pre-tension T at high braking torques (Figure 5(c)). On the other hand, at low braking torques, $\Delta M(\%)$ first slightly drops and then rises. $\Delta M(\%)$ increases with larger pulleys (Figure 5(d)) at high braking torques, but it first drops slightly and then increases at low braking torques. As shown in Figure 5(e), $\Delta M(\%)$ first decreases and then increases when a belt with a higher elastic modulus is used. $\Delta M(\%)$ increases with increasing belt length, as indicated in Figure 5(f). Longer belts are not recommended to avoid potential belt flapping, which results in energy dissipation and increased losses. A decrease in the braking torque makes this effect more pronounced.

In most test conditions, a non-linear relation exists between $\Delta M(\%)$ and the measured parameters. Tests are also conducted using more than three points, but no severe non-linearity is observed.

RSM tests

With the classical test methodology, i.e. OFAT, in order to reach conclusions similar to that of the design-of-experiments (DoE) method or RSM, too many tests need to be conducted; otherwise the conclusions would be incomplete or misleading because of an insufficient number of tests or an inappropriate test range. Individual variations can be determined using OFAT by keeping the rest of the parameters the same; however, if the interactions between the parameters are important, or the testing time and/or resources are limited, then the DoE or RSM should be utilized.[20]

RSM is a collection of statistical and mathematical techniques describing the relationship between the input parameters and the output parameters, which is useful for developing, improving and optimizing processes by using a second-order polynomial model.[21–24] In this method, a relationship between the independent input variables X_i and a response Y is obtained by fitting a second-order polynomial function. To build the empirical response models, the necessary data are generally collected by the DoE, followed by single or multiple statistical regression techniques. The validity of the empirical model is justified by the analysis of variance (ANOVA), which is a popular statistical approach based on decomposition of the total variability in the response[24] Y.

In this study, RSM is used to estimate the quantitative relationship between the key controllable variables and the response variables of the V-ribbed belt drive. The pulley diameter, the elastic modulus of the belt, the braking torque, the motor speed and the belt pre-tension are selected as the factors considered to affect the power loss behaviour of V-ribbed belt drives. On the other hand, the percentage torque loss $\Delta M(\%)$ is considered as a response. The range of values for each factor is given in Table 2. The upper limits and lower limits are chosen on the basis of our laboratory experience, physical resources and information published in the scientific literature for similar systems.

The high level in terms of the coded value is set to $+1$, and the low level to -1. The coded variables are calculated as

$$X_1 = \frac{\omega - \omega_0}{\Delta\omega}, \quad X_2 = \frac{M - M_0}{\Delta M}, \quad X_3 = \frac{T - T_0}{\Delta T}$$
$$X_4 = \frac{D - D_0}{\Delta D}, \quad X_5 = \frac{E - E_0}{\Delta E} \tag{6}$$

where X_i are the coded values of the factors ω, M, T, D and E respectively and ω_0, M_0, T_0, D_0 and E_0 are the mean values of the factors respectively. Δ indicates the difference between the maximum value and the minimum value of the respective parameter.

The experiment plan, generated in accordance with face-centred composite design, consists of 50 runs. The factorial portion is a full factorial design with all combinations of the parameters at two levels and composed of 10 central points and eight star points. The design matrix and all the corresponding results on the percentage torque losses are given in Table 3.

RSM results.

$\Delta M(\%)$ does not show a large variation over the ranges of pulley speeds and belt tensions, similar to OFAT results, as seen in Figure 6(a) and (c). Although the absolute torque losses rise with increasing braking torque, $\Delta M(\%)$ decreases with increasing braking torque, as demonstrated in Figure 6(b). The non-linear dependences of $\Delta M(\%)$ on the pulley diameter and the belt stiffness, as shown in Figure 6(d) and (e), are also in good agreement with the OFAT studies. On the other hand, the non-linearity found in the relations

Table 2. The range of values for the design factors used in RSM.

Factor	Units	High value (+1)	Low value (–1)
Motor speed ω	r/min	2040	865
Brake torque M	N m	7	3
Total belt pre-tension T	kgf	70	30
Pulley diameter D	mm	92.5	72.5
Elastic modulus E of the belt	MPa	4730	3190

Table 3. Design matrix.

Standard order		1	2	3	4	5	6	7	8	9	10	11	12	13	14	15	16	17
Run order		25	44	49	20	46	30	3	39	50	40	43	11	31	21	17	41	2
Factor 1	X_1	−1	1	−1	1	−1	1	−1	1	−1	1	−1	1	−1	1	−1	1	−1
Factor 2	X_2	−1	−1	1	1	−1	−1	1	1	−1	−1	1	1	−1	−1	1	1	−1
Factor 3	X_3	−1	−1	−1	−1	1	1	1	1	−1	−1	−1	−1	1	1	1	1	−1
Factor 4	X_4	−1	−1	−1	−1	−1	−1	−1	−1	1	1	1	1	1	1	1	1	−1
Factor 5	X_5	−1	−1	−1	−1	−1	−1	−1	−1	−1	−1	−1	−1	−1	−1	−1	−1	1
Response	Torque loss (%)	11.44	11.73	6.951	7.155	13.52	12.92	7.975	7.578	16.81	15.15	9.273	9.672	19.38	18.77	11.37	11.45	12.41
Standard order		18	19	20	21	22	23	24	25	26	27	28	29	30	31	32	33	34
Run order		36	35	32	1	42	5	22	16	26	7	48	29	33	38	4	47	27
Factor 1	X_1	1	−1	1	−1	1	−1	1	−1	1	−1	1	−1	1	−1	1	−1	1
Factor 2	X_2	−1	1	1	−1	−1	1	1	−1	−1	1	1	−1	−1	1	1	0	0
Factor 3	X_3	−1	−1	−1	1	1	1	1	−1	−1	−1	−1	1	1	1	1	0	0
Factor 4	X_4	−1	−1	−1	−1	−1	−1	−1	1	1	1	1	1	1	1	1	0	0
Factor 5	X_5	1	1	1	1	1	1	1	1	1	1	1	1	1	1	1	0	0
Response	Torque loss (%)	10.12	6.876	6.861	13.64	12.38	7.307	6.716	15.73	14.71	9.233	9.244	16.64	15.82	10.35	10.35	7.548	6.575
Standard order		35	36	37	38	39	40	41	42	43	44	45	46	47	48	49	50	
Run order		13	12	37	18	28	23	45	9	8	15	14	19	10	24	34	6	
Factor 1	X_1	0	0	0	0	0	0	0	0	0	0	0	0	0	0	0	0	
Factor 2	X_2	−1	1	0	0	0	0	0	0	0	0	0	0	0	0	0	0	
Factor 3	X_3	0	0	−1	1	0	0	0	0	0	0	0	0	0	0	0	0	
Factor 4	X_4	0	0	0	0	−1	1	0	0	0	0	0	0	0	0	0	0	
Factor 5	X_5	0	0	0	0	0	0	−1	1	0	0	0	0	0	0	0	0	
Response	Torque loss (%)	[a]	[a]	7.604	8.861	9.230	11.84	9.984	8.271	7.532	7.532	7.532	7.532	7.532	7.532	7.532	7.532	

[a]Unavailable data point.

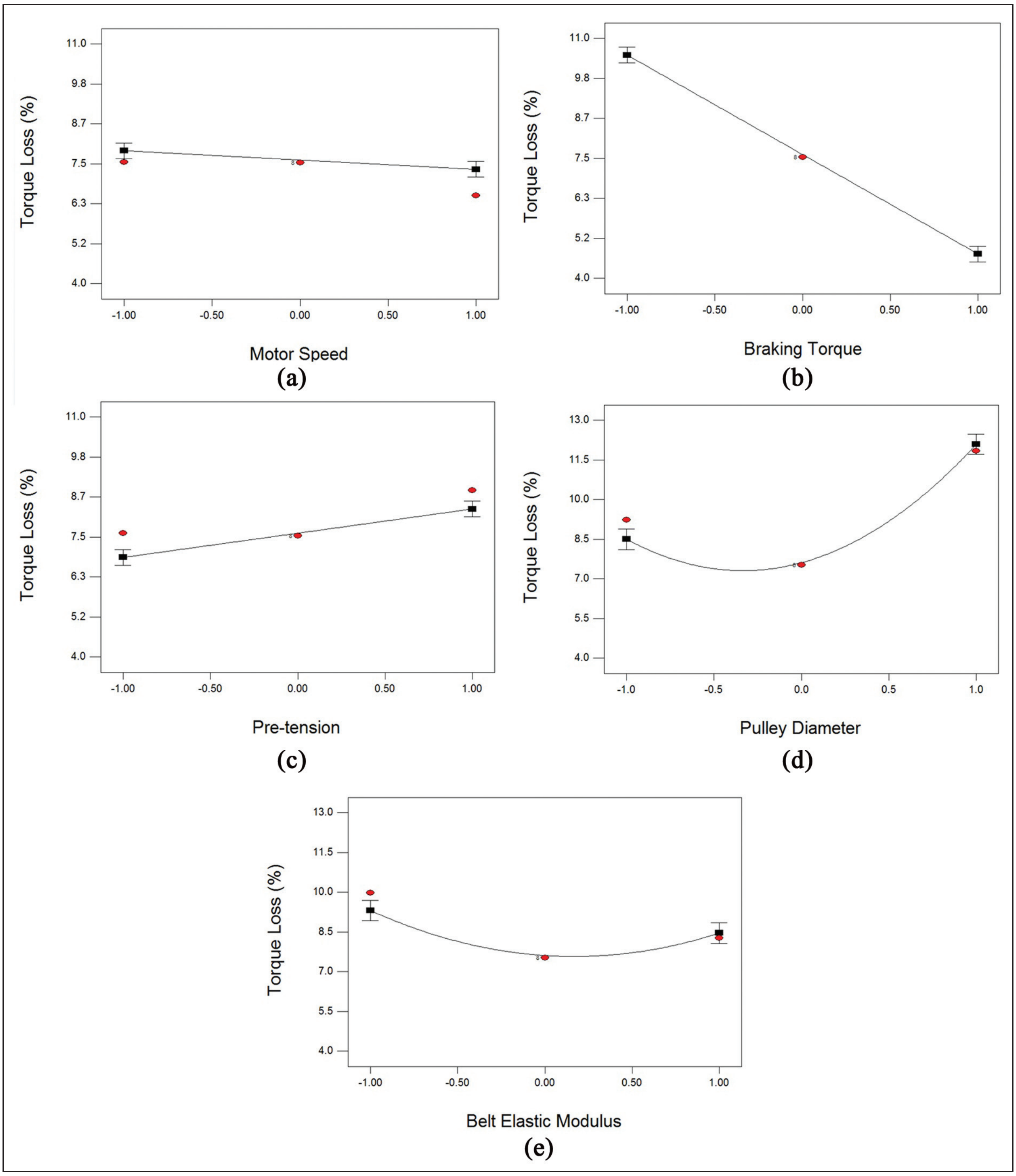

Figure 6. Effects of the individual factors on the percentage torque loss ΔM (%): (a) the motor speed ω at $E = 3960$ MPa, $M = 5$ N m, $L = 660$ mm, $T = 50$ kgf and $D = 85$ mm; (b) the braking torque M at $\omega = 1453$ r/min, $E = 3960$ MPa, $L = 660$ mm, $T = 50$ kgf and $D = 85$ mm; (c) the pre-tension T at $\omega = 1453$ r/min, $M = 5$ N m, $L = 660$ mm, $E = 3960$ MPa and $D = 85$ mm; (d) the pulley diameter D at $\omega = 1453$ r/min, $M = 5$ N m, $L = 660$ mm, $T = 50$ kgf and $E = 3960$ MPa; (e) the elastic modulus E of the belt at $\omega = 1453$ r/min, $M = 5$ N m, $L = 660$ mm, $T = 50$ kgf and $D = 85$ mm.

for the driver speed and the pre-tension in OFAT studies (Figure 5(a) and (c)) is not found to be statistically significant by RSM (Figure 6(a) and (c)), given the variations in the test data.

Figure 7 presents the dependence of the response surface of $\Delta M(\%)$ on various parameters. There is an almost linear interaction between the braking torque and the motor speed. At high braking torques, $\Delta M(\%)$ reaches the lowest values. As seen in Figure 7(b), $\Delta M(\%)$ takes its lower values at medium pulley diameters. The effect of the pre-tension on $\Delta M(\%)$ is small in comparison with that of the pulley diameter. Figure 7(c) presents the $\Delta M(\%)$ response surface for the belt pre-tension and the braking torque variables. Energy is dissipated because of hysteresis as the belt is radially compressed and released while it enters and leaves a

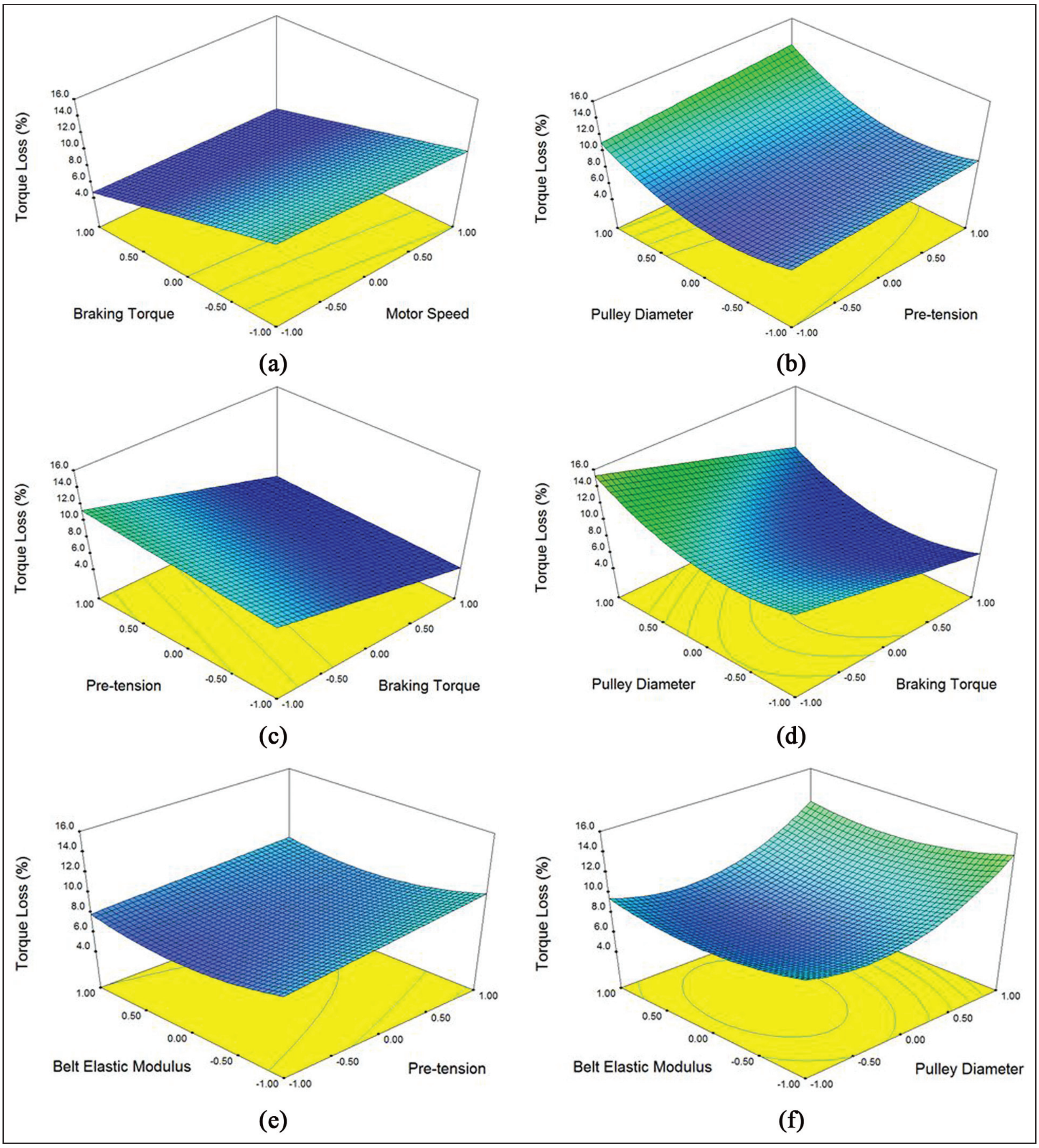

Figure 7. Response surface and contour plots of the percentage torque loss ΔM (%) versus (a) the brake torque M and the motor speed ω at $D = 85$ mm, $T = 50$ kgf, $L = 660$ mm and $E = 3960$ MPa, (b) the pulley diameter D and the pre-tension T at $\omega = 865$ r/min, $E = 3960$ MPa, $M = 5$ N m and $L = 660$ mm, (c) the pre-tension T and the brake torque M at $\omega = 865$ r/min, $D = 85$ mm, $E = 3960$ MPa and $L = 660$ mm, (d) the pulley diameter D and the brake torque M at $\omega = 865$ r/min, $T = 50$ kgf, $E = 3960$ MPa and $L = 660$ mm, (e) the elastic modulus E of the belt and the pre-tension T at $\omega = 865$ r/min, $D = 85$ mm, $M = 5$ N m and $L = 660$ mm and (f) the elastic modulus E of the belt and the pulley diameter D at $\omega = 865$ r/min, $E = 3960$ MPa, $M = 5$ N m and $L = 660$ mm.

pulley. Increasing the belt tension intensifies this effect but also reduces slipping of the belt over the pulley. Because of these counteracting effects, $\Delta M(\%)$ does not vary much with the belt tension. As Figure 7(d) indicates, the effect of the pulley diameter is more pronounced at low braking torques. As seen in Figure 7(e) and (f), the elastic modulus of the belt has a small effect on $\Delta M(\%)$, but it is non-linear. This effect is more pronounced for large pulley diameters.

ANOVA. ANOVA is a statistical method for making comparisons between the means of two or more parameters in order to determine the significant variable

Table 4. ANOVA for the percentage torque loss (after backward elimination).

Source	Sum of squares	Degree of freedom	Mean square	F value	Probability $> F$	
Model	556.82	13	42.83	181.33	< 0.0001	Significant
X_1	2.52	1	2.52	10.65	0.0025	
X_2	269.17	1	269.17	1139.47	< 0.0001	
X_3	17.01	1	17.01	71.99	< 0.0001	
X_4	109.38	1	109.38	463.04	< 0.0001	
X_5	6.15	1	6.15	26.02	< 0.0001	
X_1X_2	1.82	1	1.82	7.72	0.0088	
X_2X_3	1.58	1	1.58	6.71	0.0140	
X_2X_4	4.01	1	4.01	16.96	0.0002	
X_3X_4	1.05	1	1.05	4.43	0.0428	
X_3X_5	1.44	1	1.44	6.08	0.0188	
X_4X_5	1.46	1	1.46	6.19	0.0179	
X_4^2	25.84	1	25.84	109.38	< 0.0001	
X_5^2	5.82	1	5.82	24.93	< 0.0001	
Residual	8.03	34	0.24			
Lack of fit	8.03	27	0.30			Not significant
Pure error	0.000	7	0.000			
Corrected total	564.86	47				

Parameter	Value
Standard deviation	0.49
Mean	10.41
Coefficient of variation (%)	4.67
Predicted residual error sum of squares	17.67
R^2	0.9858
Adjusted R^2	0.9803
Predicted R^2	0.9687
Adequate precision	46.470

over the desired response. The statistical significance of each input variable on the behaviour of the percentage torque loss is presented in Table 4. If the probability $> F$ value is smaller than 0.05, the regression model is statistically significant. In contrast, probability $> F$ values greater than 0.05 are considered to be statistically insignificant, having no individual effect on the percentage torque loss. After backward elimination, Table 4 demonstrates the significant terms only. The main factors (quadratic terms as well as the interaction terms shown in the table) have probability $> F$ values less than 0.05, as indicated in Table 4; consequently, they are considered to be significant. There is no significant lack of fit in the model and the residual plots are satisfactory (see the section on model adequacy check), and so it can be concluded that the reduced model is adequate. F values represent the ranking of the significance of the terms between each other. The F value for the braking torque and the pulley diameter indicates that they are the most significant parameters over the response, i.e. the percentage torque loss.

The response surface equation for the percentage torque loss ΔM (%) is obtained in terms of the coded parameters by using Design Expert V9 software as

$$\begin{aligned}\Delta M(\%) = {} & 7.61 - 0.27X_1 - 2.9X_2 + 0.71X_3 + 1.79X_4 \\ & -0.43X_5 + 0.24X_1X_2 - 0.22X_2X_3 \\ & -0.35X_2X_4 + 0.18X_3X_4 - 0.21X_3X_5 \\ & -0.21X_4X_5 + 2.68X_4^2 + 1.27X_5^2 \end{aligned} \tag{7}$$

Furthermore, by calculating the correlation coefficient R^2, a measure of the strength of this quadratic relationship in correctly predicting $\Delta M(\%)$ can be obtained. R^2 is defined as the ratio of the sum of squares SS_R for model regression to the sum of squares SS_T for total regression. For the empirical data, R^2 is obtained to be 98.58%, which shows the closeness of the predicted values to the experimental data. This value indicates that the model will predict future data quite well.

Optimization of design parameters

After finding the functional relationships between the key controllable variables and response variables, it is possible to optimize the response.[24] In this study, an automotive application is considered for optimization.

Case study

The power loss is a critical factor in belt-drive systems such as front-end accessory drives (FEADs) in automotive vehicles especially in high-accessory-load and low-speed conditions, such as the use of air conditioning or an alternator unit at the start or stop. The optimization problem in this case study is to find the optimal values of the design parameters for minimum torque loss in harsh operating conditions subjected to the constraints on the values of the variables. This single-objective problem can be stated as

$$\text{Minimize}\,\Delta M\,(\%) = \text{percentage torque loss} = f(\omega, M, T, D, E)$$

subject to

$$\begin{aligned} &865\,\text{r/min} \leqslant \omega \leqslant 1453\,\text{r/min} \\ &6\,\text{Nm} \leqslant M \leqslant 7\,\text{Nm} \\ &30\,\text{kgf} \leqslant T \leqslant 70\,\text{kgf} \\ &72.5\,\text{mm} \leqslant D \leqslant 92.5\,\text{mm} \\ &3190\,\text{MPa} \leqslant E \leqslant 4730\,\text{MPa} \\ &\text{for } L = 660\,\text{mm} \end{aligned} \tag{8}$$

A typical high-load accessory unit in a FEAD system consumes about 6–7 N m load from the crankshaft. For that reason, in this case study, the braking torque takes values limited to 6–7 N m. The speed range was selected as 865–1453 r/min referring to the idle speed and the alternator engagement speed of an automotive engine application. The same upper limits and lower limits are used for the pre-tension, the pulley diameter and the elastic modulus of the belt in the design optimization as in the response surface analysis, and the length of the belt is taken to be a constant parameter.

In order to maximize the objective function, a direct search method is used. The optimal setting that minimizes $\Delta M(\%)$ within the selected ranges is listed in Table 5. It can be observed that use of soft belts under a low belt tension, together with small pulley diameters run at low motor speeds and high braking torques apparently reduces the percentage torque loss in the harsh operating conditions of a typical FEAD system.

Confirmation experiment for model verification

In order to verify the optimum results obtained via RSM and the response function, an additional test is performed on the test bench with the optimum conditions listed in Table 5. The confirmation experiment reveals that the difference between the predicted value for $\Delta M(\%)$ and the experimental value is 8.5%. It may be concluded that the proposed model for the percentage torque losses in V-ribbed belt drives is reasonably accurate.

Table 5. Optimal settings for the minimized percentage torque loss under critical operating conditions.

Parameter	Optimal setting
Motor speed ω	−0.95
Brake torque M	0.99
Total belt pre-tension T	−0.95
Pulley diameter D	−0.90
Elastic modulus E of the belt	−0.90
Torque loss	6.4

Model adequacy check

The adequacy of the experimental designs is checked to confirm that the models have extracted all the relevant information from the experimental data, and to ensure that the regression equation provides a sufficient approximation of the true system.[24] The primary diagnostic tool for this purpose is the residual analysis.[20, 25, 26] The residuals are defined as the differences between the actual values and the predicted values of response corresponding to each design. The residual results are shown in Figure 8.

If a model is adequate, first the residuals should have a normal distribution. The vertical axis of Figure 8(a) is the probability scale and the horizontal axis is the data scale. A least-squares line is then fitted to the plotted points. The line forms an estimate of the cumulative distribution function for the population from which data are drawn. When the P value is smaller than 0.05, it will be classified as significant and the null hypothesis has to be rejected. The P value in Figure 8(a) is larger than[20] 0.05; thus, the residuals for the percentage torque loss values follow a normal distribution, and the predictive regression model at the final stage of the study has extracted all the available information from the experimental data. The rest of the information defined as residuals can be considered as errors resulting from the experiments.

Figure 8(b) represents the fitted value plot, where the values predicted by the response curve are on the horizontal axis and the differences between the actual values and predicted values are on the vertical axis. The fitted value plot should represent equal variance levels around the centre-line, which corresponds to 'zero' residual value, as shown in Figure 8(b).

Figure 8(c) represents the order of the data plot, where the order of the observed data, or the run order in Table 3, is shown on the horizontal axis and the residual values are given on the vertical axis similar to the fitted value plot. The measurements should not affect subsequent measurements or the set-up should not produce data showing any significant trend over time. The measured data in the present study can be considered to be adequate in this respect.

Conclusions

In this study, a test bench is constructed to determine the effects of the pulley diameter, the pulley speed, the belt length, the belt pre-tension, the belt material and the braking torque on the torque loss in V-ribbed belt drives. Because the torque measurements are not taken directly at the pulleys but at the motor housing and the dynamometer housing, the measured values also include the idling torque losses at the motor and the

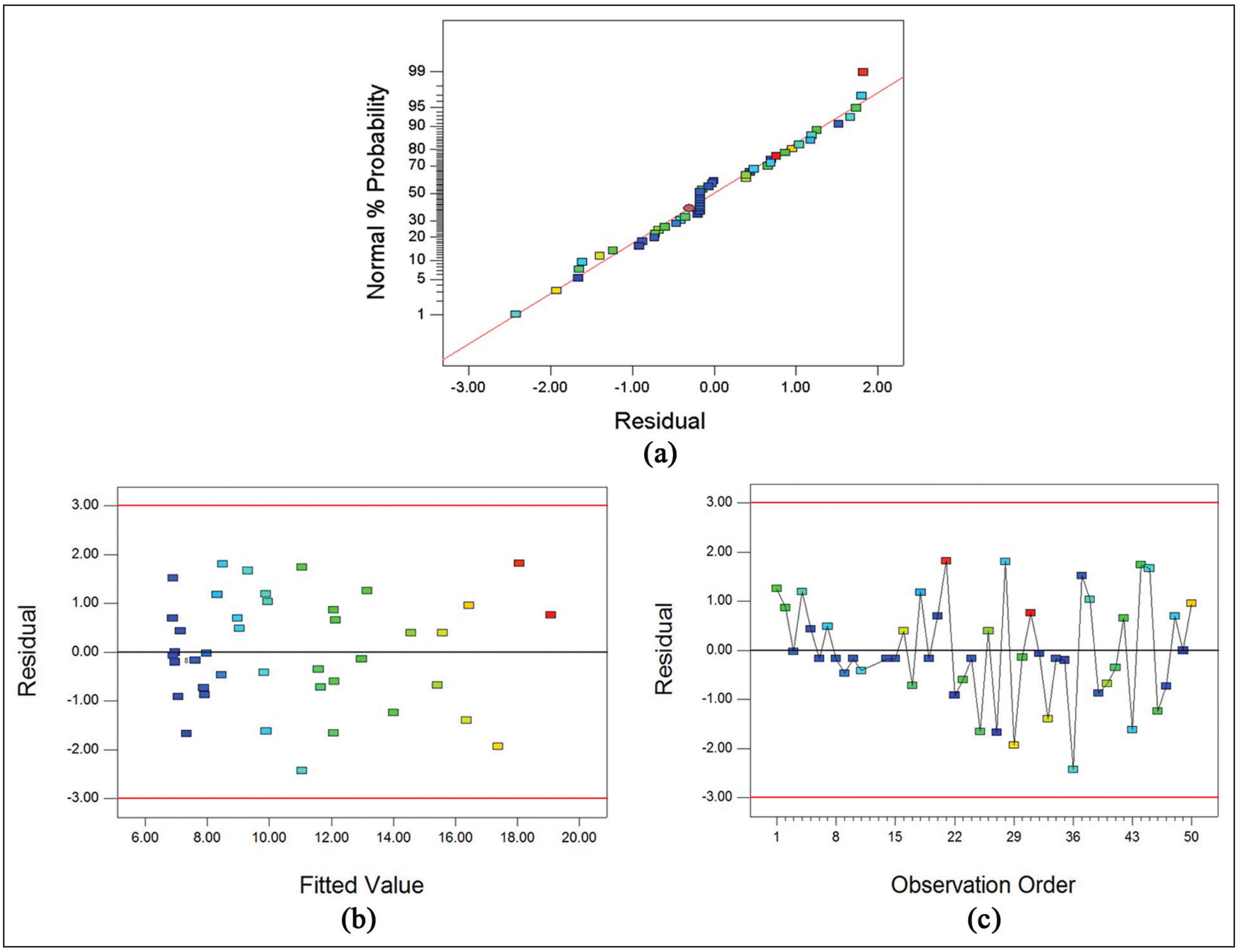

Figure 8. Adequacy check for the response surface design: (a) normal distribution plot of the residuals; (b) fitted value plot for ΔM (%); (c) observation order plot of residuals for ΔM (%).

dynamometer, which become evident when the motor is run with no belt installed. While no torque is being transmitted to the driven pulley, a torque is still needed to run the motor. In this study, the idling torque loss is also measured and subtracted from the measured torque loss values; then, the percentage difference is calculated to find the net percentage torque loss. OFAT and RSM are used to find the effects of the belt-drive parameters on the torque loss.

The factors that have most effect on the percentage torque losses are found to be the braking torque and the pulley diameter, while the factor with the least effect is the pulley speed. Although an increased braking torque leads to an increase in the absolute torque loss values, when the percentage torque losses are concerned, this behaviour is reversed. For a given belt length, an intermediate size for the pulley diameter results in the minimum torque loss. A similar observation can also be made for the elastic modulus. Longer belts result in increased percentage torque loss, which may be due to the increased effect of belt flapping.

Response surface plots indicate the influencing parameters and their effects on the percentage torque loss. Response surface analysis clearly shows that the parameters have interactions between themselves and that non-linearity exists. The adequacy of the models is checked and verified by conducting an ANOVA. Usually the motor speed and the braking torque have pre-defined values at the beginning of a belt-drive design, but it is possible to find the optimum operating conditions using the equations derived by RSM. A case study is considered, in which the belt-drive parameters are optimized. An experiment is then conducted using the optimum parameter values. The error between the predicted values and the measured values of torque loss turned out to be 8.5%. This value can be considered to be small.

Acknowledgement

We would like to thank Mehmet Uçar and Bülent Balta for their valuable support during this study. We would also like to thank to Teklas AŞ where stiffness measurements were performed.

Declaration of conflict of interest

The authors declare that there is no conflict of interest.

Funding

This research received no specific grant from any funding agency in the public, commercial or not-for-profit sectors.

References

1. Almeida A and Greenberg S. Technology assessment: energy-efficient belt transmissions. *Energy Buildings* 1995; 22(3): 245–253.
2. http://simplybearings.co.uk/shop/Belts-Multi + Ribbed + Poly-V + Belts/c4601_4791/index.html High Quality Branded Poly-V multi ribbed v-belts in all sections. Accessed: 13 October 2014.
3. Gerbert G. Belt slip – a unified approach. *Trans ASME, J Mech Des* 1996; 118: 432–438.
4. Peek H and Fischer F. Experimental investigation of power loss and operating conditions of statically loaded belt drives. In: *1989 international power transmission and gearing conference new technologies for power transmissions of the 90's*, Chicago, Illinois, USA, 25–29 April 1989, pp. 15–24. New York: ASME.
5. Childs THC and Cowburn D. Power transmission losses in V-belt drives Part 1: mismatched belt and pulley groove wedge angle effects. *Proc IMechE Part D: J Automobile Engineering* 1987; 201(1): 33–40.
6. Childs THC and Cowburn D. Power transmission losses in V-belt drives Part 2: effects of small pulley radii. *Proc IMechE Part D: J Automobile Engineering* 1987; 201(1): 41–53.
7. Ferrando F, Martin F and Riba C. Axial force test and modeling of the V-belt continuously variable transmission for mopeds. *Trans ASME, J Mech Des* 1996; 118: 266–273.
8. Amijma S, Fujii T, Matuoka H and Ikeda E. Study on axial force and its distribution for a newly developed block-type CVT belt. *Int J Veh Des* 1991; 12: 324–335.
9. Chen TF, Lee DW and Sung CK. An experimental study on transmission efficiency of a rubber V-belt CVT. *Mech Mach Theory* 1998; 33: 351–363.
10. Akehurst S, Vaughan ND, Parker DA and Simmer D. Modeling of loss mechanisms in a pushing metal V-belt continuously cariable transmission Part 1: torque losses due to band friction. *Proc IMechE Part D: J Automobile Engineering* 2004; 218(11): 1269–1281.
11. Akehurst S, Vaughan ND, Parker DA and Simmer D. Modeling of loss mechanisms in a pushing metal V-belt continuously variable transmission Part 2: pulley deflection losses and total torque loss validation. *Proc IMechE Part D: J Automobile Engineering* 2004; 218(11): 1283–1293.
12. Akehurst S, Vaughan ND, Parker DA and Simmer D. Modeling of loss mechanisms in a pushing metal V-belt continuously variable transmission Part 3: belt slip losses. *Proc IMechE Part D: J Automobile Engineering* 2004; 218(11): 1295–1306.
13. Dalgarno KW, Moore RB and Day AJ. Tangential slip noise of V-ribbed belts. *Proc IMechE Part C: J Mechanical Engineering Science* 1999; 213: 741–749.
14. Yu D, Childs THC and Dalgarno KW. Experimental and finite element studies of the running of V-ribbed belts in pulley grooves. *Proc IMechE Part C: J Mechanical Engineering Science* 1998; 212: 343–355.
15. Yu D, Childs THC and Dalgarno KW. V-ribbed belt design, wear and traction capacity. *Proc IMechE Part D: J Automobile Engineering* 1998; 212(4): 333–344.
16. Xu M, Castle JB, Shen Y and Chandrashekhara K. Finite element simulation and experimental validation of V-ribbed belt tracking. SAE paper 2001-01-0661, 2001.
17. Manin L, Michon G, Remond D and Dufour R. From transmission error measurement to pulley-belt slip determination in serpentine belt drives: influence of tensioner and belt characteristics. *Mech Mach Theory* 2009; 44: 813–821.
18. Cepon G, Manin L and Boltezar M. Experimental identification of the contact parameters between a V-ribbed belt and pulley. *Mech Mach Theory* 2010; 45: 1424–1433.
19. Balta B, Balta B, Sonmez FO et al. Torque loss measurements on V-ribbed belts. In: *ASME 2012 11th biennial conference on engineering systems design and analysis, Vol 3: advanced composite materials and processing; robotics; information management and PLM; design engineering*, Nantes, France, 2–4 July 2012, paper ESDA2012-82245, pp. 591–595. New York: ASME.
20. Montgomery DC. *Design and analysis of experiments*. 5th edition. New York: John Wiley, 2001.
21. Chen C, Su P and Lin Y. Analysis and modeling of effective parameters for dimension shrinkage variation of injection molded part with thin shell feature using response surface methodology. *Int J Advd Mfg Technol* 2009; 45: 1087–1095.
22. Reisgen U, Schleser M, Mokrov O and Ahmed E. Statistical modeling of laser welding of DP/TRIP steel sheets. *Optics Laser Technol* 2012; 44: 92–101.
23. Reisgen U, Schleser M, Mokrov O and Ahmed E. Optimization of laser welding of DP/TRIP steel sheets using statistical approach. *Optics Laser Technol* 2012; 44: 255–262.
24. Myers RH and Montgomery DC. *Response surface methodology*. 2nd edition. New York, John Wiley 2002.
25. Breyfogle FW. *Implementing six sigma. Smarter solutions using statistical methods*. 2nd edition. Hoboken, New Jersey: John Wiley, 2003.
26. Six Sigma Academy. *The black belt memory jogger*. 1st Edition. Salem, New Hampshire: GOAL/QPC and Six Sigma Academy, 2002